

Compensation methods using a new model for buried defects in extreme ultraviolet lithography masks

Chris H. Clifford^{1,2*}, Tina T. Chan¹, Andrew R. Neureuther¹
Ying Li², Danping Peng², Linyong Pang²

¹Department of Electrical Engineering and Computer Sciences, University of California, Berkeley, CA 94720

²Luminescent Technologies, Inc., 2471 East Bayshore Road, Suite 600, Palo Alto, CA 94303

ABSTRACT

A new method for predicting the reflection from an extreme ultraviolet (EUV) multilayer is described which when implemented into the new Defect Printability Simulator (DPS) can calculate the image produced by an EUV mask with a buried defect several orders of magnitude faster than the finite difference time domain (FDTD). A new buried defect compensation method is also demonstrated to correct the in focus image of a line space pattern containing a buried defect.

The new multilayer model accounts for the disruption of the magnitude and phase of the reflected field from an EUV multilayer defect. It does this by sampling the multilayer on a non-uniform grid and calculating the analytic complex local reflection coefficient at each point. After this step, the effect of the optical path difference due to the surface defect profile is added to the total reflected field to accurately predict the reflected magnitude and phase at all points on the multilayer surface.

The accuracy of the new multilayer model and the full DPS simulator is verified by comparisons to FDTD simulations. The largest difference between the two methods was 0.8nm for predicting the CD change due to a buried defect through focus. This small difference is within the margin of error for FDTD simulations of EUV multilayers. The runtime of DPS is compared to extrapolated FDTD runtimes for many simulation domain sizes and DPS is 4-5 orders of magnitude faster for all cases. For example, DPS can calculate the reflected image from a 1 μ m x 1 μ m mask area in less than 30 seconds on a single processor. FDTD would take a month on four processors.

The new compensation strategy demonstrated in this work is able to remove all CD error in the simulated image due to a buried defect in a 22nm dense line space pattern. The method is iterative and a full DPS simulation is run for every iteration. After each simulation, the absorber pattern is adjusted based on the difference of the thresholded target image and thresholded defective image. This method is very simple and does not attempt to compensate for the defect through focus, but it does demonstrate the usefulness of a fast simulator for compensation.

Keywords: fast simulation, buried defect, EUV mask, defect compensation

1. INTRODUCTION

Extreme ultraviolet (EUV) lithography is the leading candidate to replace optical lithography for semiconductor patterning. However, there are many issues which are delaying implementation of the technology and may prevent its implementation altogether. One of the most critical problems is mask defects, specifically buried multilayer defects, which are unique to EUV masks. This paper introduces a new multilayer model, a new fast simulator and a simple defect compensation algorithm to help reduce the mask defect problem.

After this introduction, the next section of this paper gives more motivation for fast EUV mask simulations. Section 3 describes the new multilayer model and overall EUV mask simulation methodology. The new simulator described in this paper is called Defect Printability Simulator (DPS) and is based on the RADICAL simulator developed at the University of California – Berkeley. In sections 4 and 5 the accuracy and speed are analyzed. DPS is 4-5 orders of magnitude faster than the finite difference time domain (FDTD) method, but has comparable accuracy. The final section demonstrates an application of DPS for defect compensation. The simulated effect of a multilayer defect on an in focus thresholded wafer image is totally eliminated by changes to the absorber pattern near the defect

*cclifford@luminescent.com; phone: (651) 238-9628

2. MOTIVATION

Buried defects in EUV mask multilayers are a major problem which must be solved before extreme ultraviolet lithography can be implemented. As Figure 1 shows, a substrate defect causing a very small multilayer surface bump can have an unacceptable effect on the final wafer image. It is unlikely that defect free EUV multilayers will be available for production EUV lithography. There have been many proposals for producing quality masks from defective multilayers, and each one requires accurate simulation of the mask image due to the pattern and buried defect. Rigorous methods, such as the finite difference time domain (FDTD), are accurate. But, these methods are too slow to be useful for most simulation applications. This paper describes a new multilayer model that has been integrated into a new simulator for EUV masks with buried defects. This new model is much faster than FDTD while maintaining comparable accuracy.

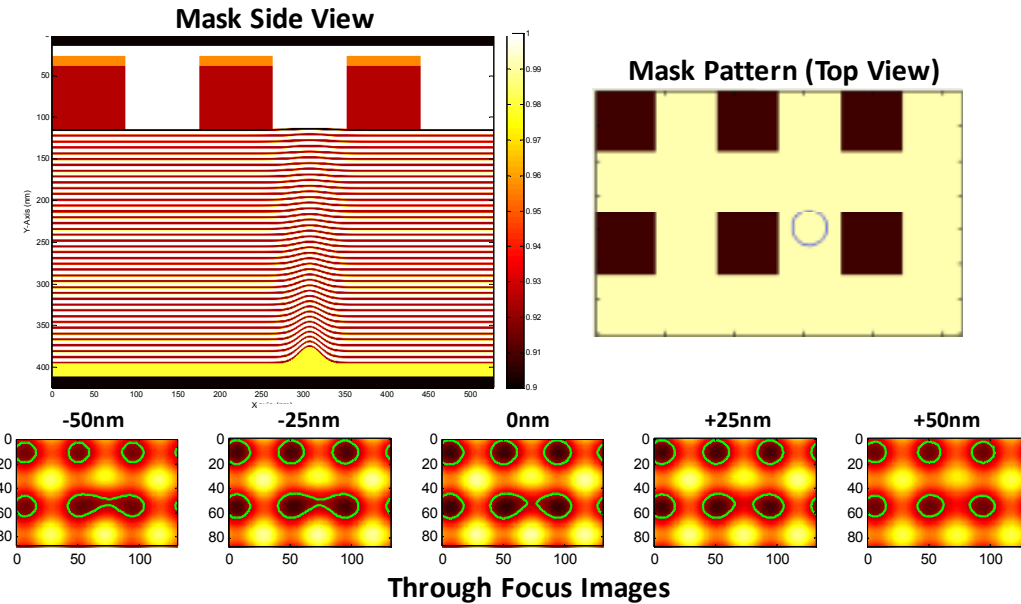


Figure 1. Example of defective EUV multilayer geometry, mask pattern, and resulting through focus wafer images.

3. SIMULATION METHODOLOGY

Full Defect Printability Simulator (DPS) Algorithm

The overall simulation flow for the Luminescent Defect Printability Simulator (DPS) is based on the simulator RADICAL developed at the University of California, Berkeley [1]. DPS is designed specifically for the simulation of EUV masks with buried defects. Therefore, each component of the simulator is optimized to be fast and accurate for the physical geometry it models, which allows significant speed increases compared to other electromagnetic simulation methods.

The overall simulation flow is summarized in Figure 2. The first step is to simulate the propagation of the incident plane wave through the absorber pattern. The resulting nearfield is Fourier transformed to produce a set of plane waves. Each plane wave in this set is simulated individually by the multilayer simulator and the results of all of the simulations are summed to produce the final field reflected from the multilayer. There are two simulation methods available in DPS: the new model presented in this paper and the advanced single surface approximation used in [1]. This result is then Fourier transformed to produce a set of plane waves which are each independently simulated through the absorber simulator. The results of each absorber simulation are summed to produce the final field reflected from the mask. The wafer image is then formed from this field using standard image calculation methods. In this paper, a new method for the multilayer simulation component of DPS is presented which is faster and more flexible than the ray tracing method used in RADICAL.

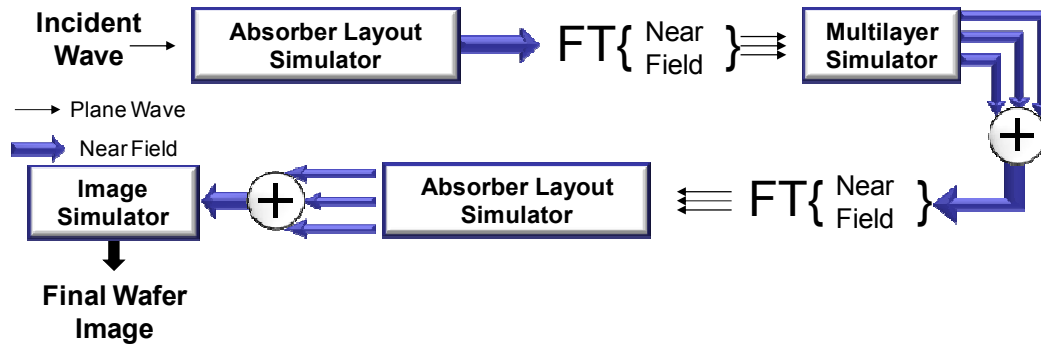


Figure 2. Defect Printability Simulator (DPS) block diagram.

Multilayer Simulation Model

For the RADICAL simulation program presented in [1], two multilayer simulation methods were available: the ray tracing method developed by Lam [2] and the single surface approximation (SSA) proposed by Gullikson [3]. In [1], the accuracy of RADICAL was comparable for both methods. But, further investigation showed that SSA was inaccurate for some multilayer geometries with defect smoothing [4]. Also, some of the assumptions made in the ray tracing algorithm break down for higher angles of incidence or large buried defects. These errors would cause the entire RADICAL program to crash in some cases. Therefore, a new model is needed.

The new model, to replace ray tracing and improve on SSA when the full multilayer geometry is known, has four steps:

1. Discretize the surface of the multilayer into square cells
2. Calculate the local analytic reflection for each cell at the input incident angle and polarization. This is the reflection from an infinite stack with the same multilayer dimensions as the cell column of the multilayer below the cell
3. Adjust the phase to account for the optical path difference due to the defect
4. Shift the Fourier transform of the field to account for the incident angle

Most multilayer simulation geometries have a localized defect, so calculating the reflection from every cell is a waste of time. Non-uniform sampling saves the calculation of the defect free multilayer reflection from being repeated unnecessarily.

4. ACCURACY

In this section, the accuracy of the new multilayer simulation method and the overall Defect Printability Simulator will be verified by comparisons to other non-rigorous methods and the finite difference time domain (FDTD). In this work, FDTD is considered to be exactly accurate, and any deviation from the FDTD results is referred to as an error. But in reality, FDTD is not exactly correct because of errors like numerical dispersion and inaccuracies in the simulation geometry inherent in modeling continuous shapes with a grid. Figure 3 shows the change in the FDTD simulated reflection coefficient from an EUV multilayer, with no features or defect, compared to the analytic value. The FDTD simulations used for comparison in this work had a cell density of 0.25nm for the 2D simulations and 0.32 for the 3D simulations. So, as Figure 3 shows, there is still some error in the FDTD results for the cell sizes used in the comparison simulations for this work. Therefore, if the error in DPS compared to FDTD is only 2-3% it will be considered an accurate result. It is important to note that although the nominal angle of incidence on an EUV mask is 6°, some light is diffracted by the absorber pattern at higher angles so FDTD and DPS must be able to simulate these angles accurately. Berkeley TEMPEST 6.1 was the FDTD program used in this work.

Simulation Parameters

There are several assumptions and parameters which apply to all simulations in the work. The EUV multilayer has 40 bilayers of alternating Silicon and Molybdenum with a 2.5nm thick Ruthenium capping layer designed for maximum reflection of 13.5nm light at 6°. The absorber is composed of two materials, a 75nm tall TaN layer and a 12nm anti-reflective layer. All line space simulations assume 6° incident light perpendicular to the direction of the lines.

Wafer image calculations assume $NA=0.32$, $\sigma=0.75$ and a 4x reduction system. For critical dimension (CD) measurements, a constant threshold which produces the correct CD for a defect free in focus simulation is used.

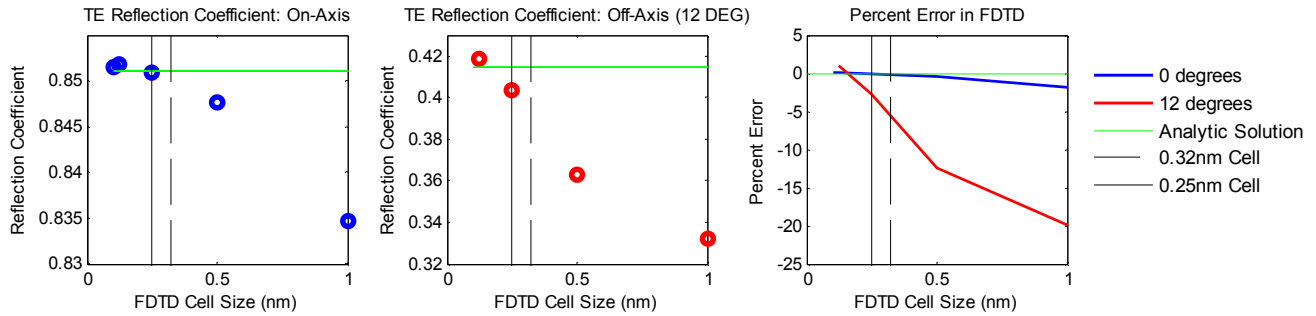


Figure 3. Plots of reflection coefficient from an EUV multilayer and error as a function of FDTD cell size for two angles of incidence compared to the exactly correct analytic solution.

New Multilayer Simulation Method Accuracy

As described above, many simulation methods are available for EUV multilayer defect simulation if there are no absorber features present. In the section, the results of four simulation methods are compared. The list below goes from least rigorous to most rigorous:

1. Advanced Single Surface Approximation (ASSA). The implementation of SSA used in [1].
2. New method presented in this paper (LUMI)
3. Ray Tracing method from [2] (RT)
4. Finite Difference Time Domain (FDTD)

To test the accuracy of the new model in different cases, the substrate height of a buried defect and angle of incidence were varied. The surface height remained constant at 2nm, so varying the substrate height effectively varied the degree of smoothing. Because, in DPS, the results of the multilayer simulation are Fourier transformed the Fourier transform of the results of each method, specifically the orders that will enter the final scanner pupil, are compared. Three accuracy cases are highlighted in Figure 4 to show how changing each parameter affects the accuracy. A summary of the accuracy is presented in Figure 5. Because 3D FDTD simulations are very time consuming, only 2D simulations are performed in this section.

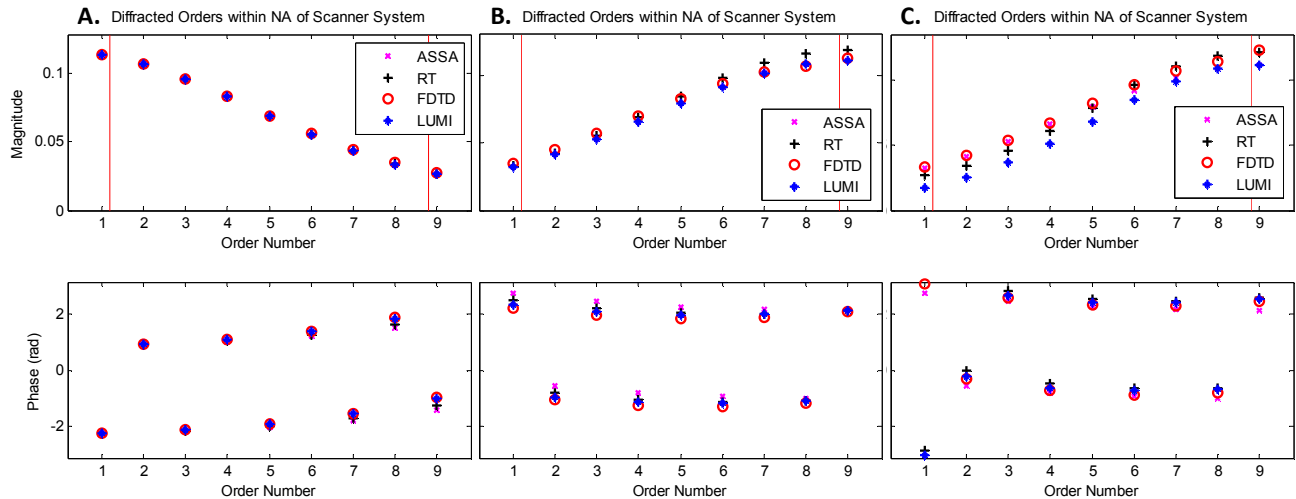


Figure 4. Comparison of diffracted orders which are collected by scanner system from an EUV multilayer defect for the four simulation types and three defect scenarios. All defects have a surface height of 2nm and a substrate and surface full width half max (FWHM) of 50nm. The differences between the three simulations are: A. Substrate height 2nm (i.e. no multilayer smoothing) and a plane wave incident at 0°, B. Substrate height 2nm (i.e. no multilayer smoothing) and a plane wave incident at 10.8°. C.) Substrate height 25nm (i.e. significant multilayer smoothing) and a plane wave incident at 10.8°.

Plot A. in Figure 4 shows a great match between all methods, with a small variation in phase for ASSA and RT. Plot B. shows that the new method actually matches FDTD better than RT overall. For C, all of the non-rigorous methods have some error. LUMI matches the phase best while RT matches the magnitude best.

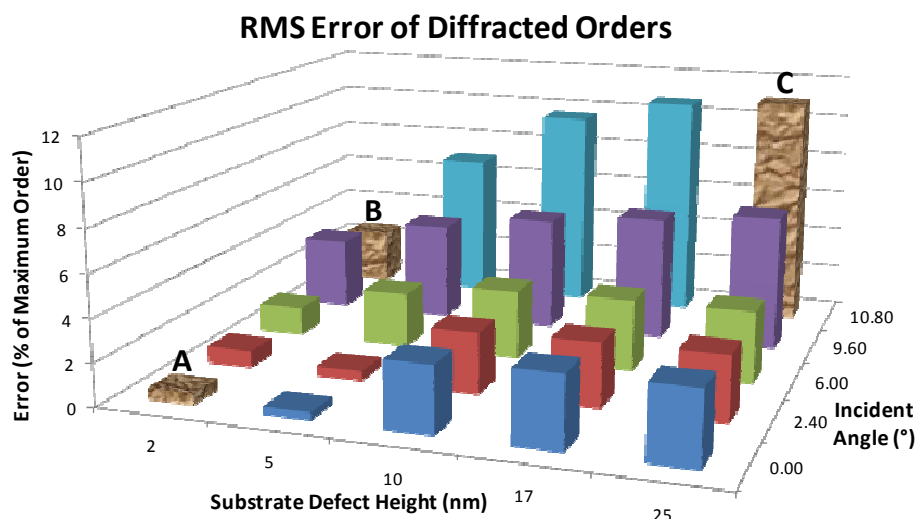


Figure 5. Summary root mean square error for several multilayer geometries. The geometries highlighted in Figure 4 are highlighted by textured bars and labels.

The accuracy of the model decreases for larger substrate defects and incident angles. This is expected based on the model described above. The error increases with angle of incidence because the assumption that the reflection from a point on the multilayer surface can be modeled by the multilayer spacing directly below it becomes less valid. The accuracy decreases with substrate defect height because the model does not account for the slight spreading of the effect of bump defects and the focusing of the effect of pit defects which occurs as light propagates into and out of the multilayer.

Additions can be made to the model to improve the accuracy if needed. But, as the next section shows small accuracy errors in certain cases for the multilayer model do no hurt the accuracy of the final aerial image.

Overall Defect Printability Simulator Accuracy

The overall Defect Printability Simulator (DPS) accuracy was verified by comparisons to 2D and 3D FDTD simulations. Because the standard output of DPS is an aerial image, the aerial image was compared between FDTD and DPS. Several 2D simulations were performed with various substrate defect sizes, defect locations, and with or without multilayer smoothing. All simulations were for defects within a dense 22nm line space pattern (1x wafer scale) Several sets of results are shown in Figure 6. These results are typical of all of the 2D simulations performed.

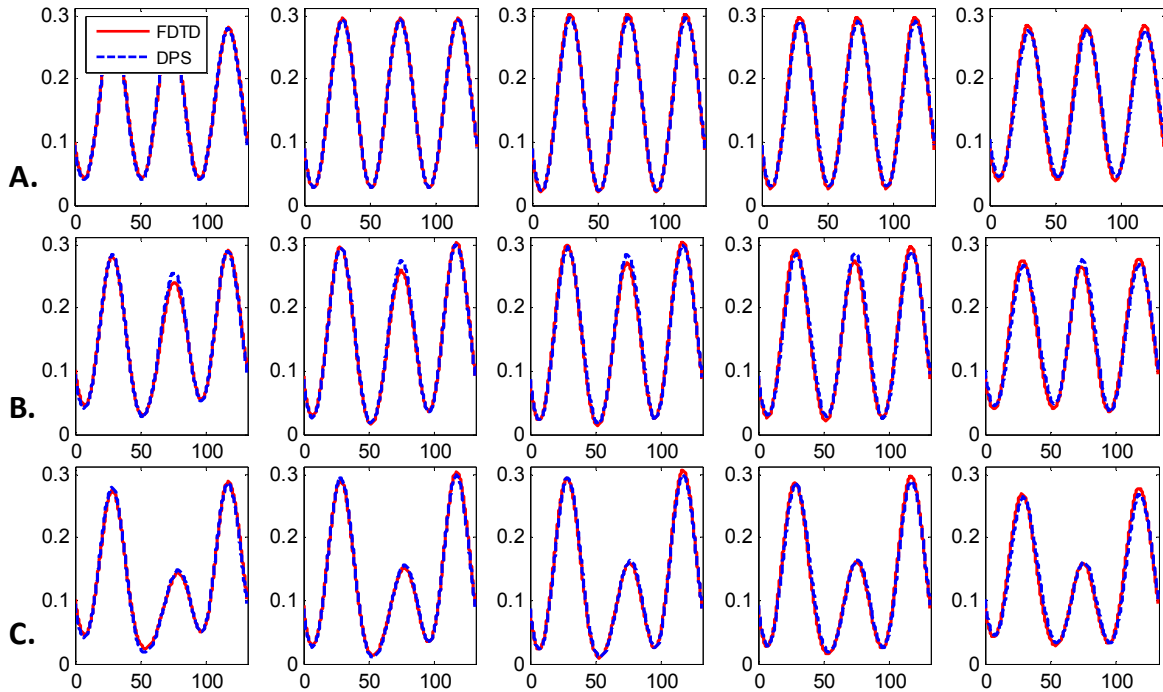


Figure 6. Aerial image cutline comparison for the three geometries. A.) Defect Free Image, B.) 1.5nm defect with uniform layers 22nm (4x) from non-shadowed edge C.) 15nm substrate defect causing a 1.5nm surface defect 22nm from non-shadowed edge

The match in Figure 6 is very good between the two methods. There are small differences, but these are within the margin of error of FDTD discussed above.

A comparison was also performed between a three-dimensional FDTD simulation and a three-dimensional DPS simulation. Because FDTD is so computationally intensive, only a small EUV mask area could be simulated. The geometry simulated in FDTD and DPS is summarized in Figure 7 and the results are shown in Figure 8 and Figure 9.

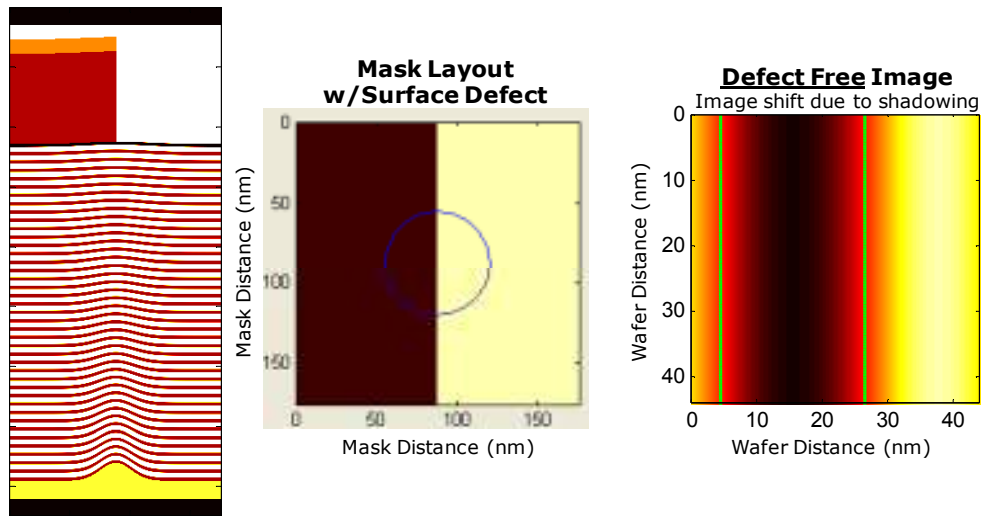


Figure 7. 3D Geometry simulated by FDTD and DPS along with defect free reference image.

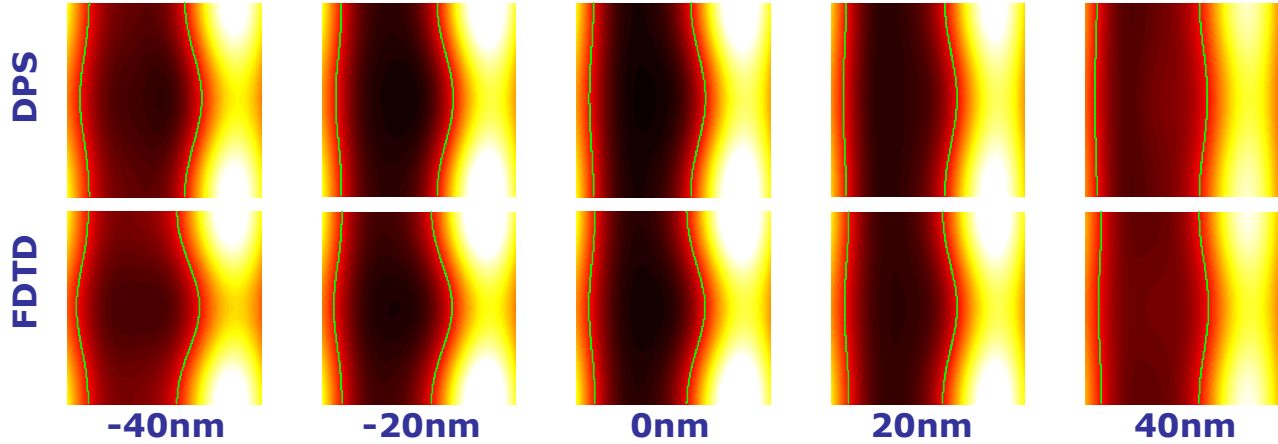


Figure 8. Wafer images through focus for FDTD and DPS

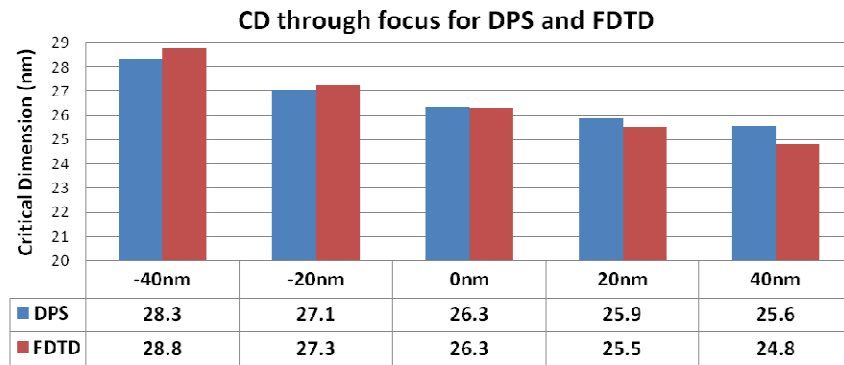


Figure 9. Comparison of measure CD for DPS and FDTD through focus.

As with the 2D simulations, there are differences between FDTD and DPS. But, these differences are very small and within the uncertainty range of the FDTD simulations. Therefore, the conclusion of this accuracy analysis is that DPS has comparable accuracy to FDTD.

5. SPEED

The Defect Printability Simulator (DPS) described in this paper was created because conventional simulation methods were too slow for defective EUV mask simulation. Since DPS was designed specifically for EUV masks with buried defects it is able to simulate these geometries much faster than more general methods. The runtimes for DPS and FDTD for a simulation the size of the 3D geometry simulated in the accuracy section above are summarized in Table 1.

	DPS with Top Surface Approximation	DPS with Full Multilayer Simulation	FDTD 42 cells/wavelength
Periodic Pattern	0.28s	0.42s	29.1 hours
Arbitrary Pattern	0.34s	0.80s	29.1 hours

Table 1. Summary of runtimes for DPS and FDTD for a 176nmx176nm mask area

As Table 1 shows, DPS can be over 100,000 times faster than FDTD. It also shows that the runtime of DPS depends on the absorber pattern simulated as well as the method used to simulate the multilayer. The runtime of DPS

depends on the number of meaningful diffraction orders from the downward propagation through the absorber pattern, because each order requires one run of the multilayer simulator. If the absorber pattern is periodic in the X and Y directions, it produces fewer diffraction orders and therefore can be simulated more quickly by DPS. The dependence on multilayer simulation methods is simple. The full multilayer model presented in this paper considers each layer below the surface of the multilayer and therefore runs slower than the advanced single surface approximation. The increase in DPS runtime as a function of mask area is summarized in Figure 10 along with an approximation of the corresponding FDTD runtime. It shows that DPS is consistently 4-5 orders of magnitude faster than FDTD.

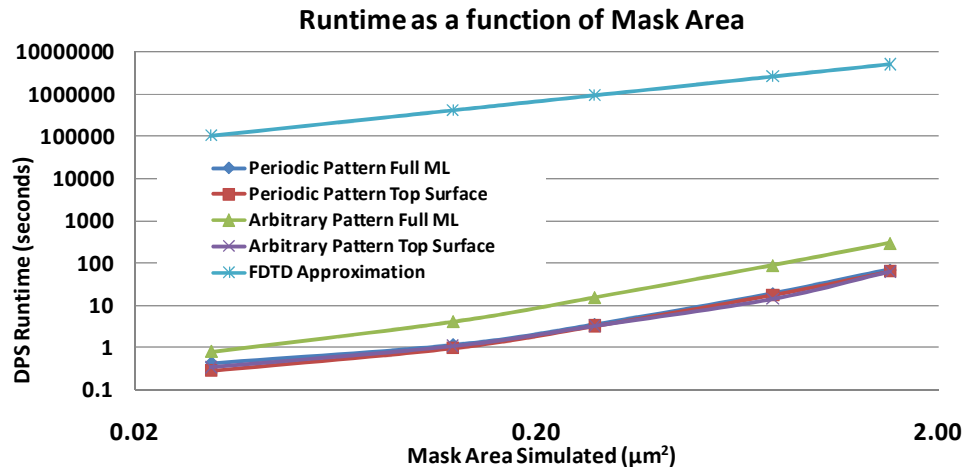


Figure 10. Comparison of runtimes for four the DPS scenarios and the predicted runtime of FDTD.

6. DEFECT COMPENSATION

It is unlikely that EUV multilayers will be available when EUV goes into production that meet the defect specifications. Therefore, some method is required to create a useable mask from a multilayer with buried defects. One possible method is to reduce EUV defect printability by changing the absorber pattern to compensate for the buried defect. A simple iterative method to compensate for defects is described in this section and summarized in Figure 11. Without the speed of DPS, this compensation algorithm would take many days on a large cluster to complete.

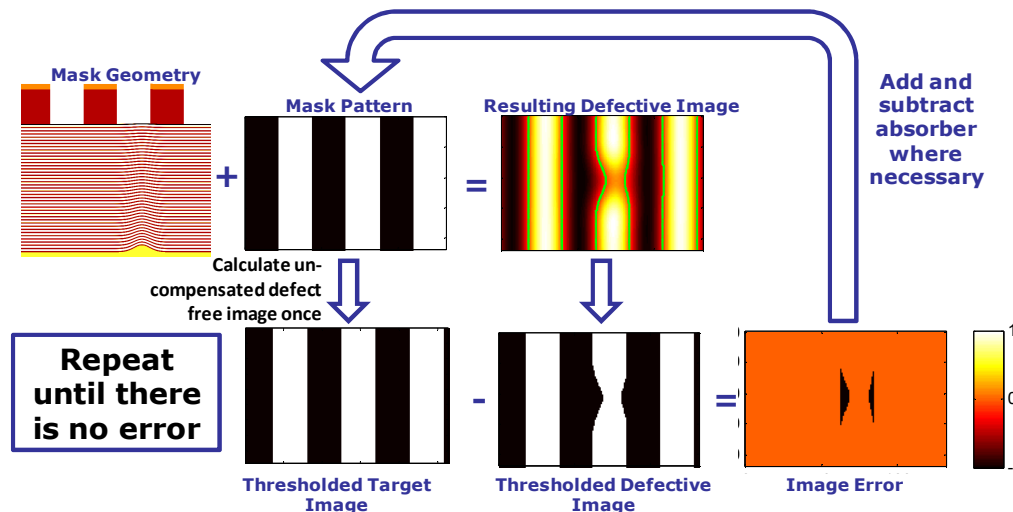


Figure 11. Summary of compensation algorithm for line space pattern with a buried defect.

As Figure 11 shows, the modifications to the absorber are determined by the point-by-point difference between the thresholded target image and current image. This is referred to as the image error. The algorithm scans each row of the image error, finds the non-zero cells, then removes or adds to the nearest absorber line edge an amount corresponding to a fraction of the image error.

An example defect to be compensated for is shown in Figure 12. As the original uncompensated image shows, the defect causes the pattern to bridge and is absolutely unacceptable. Figure 13 shows the intermediate compensated patterns after each iteration. The entire compensation process took 85 seconds. Although there are several iterations, it appears to generally be a two step process. The first step, which is mostly completed by the first iteration, is to compensate for the defect by removing absorber. The second step is to compensate for the compensation. Comparing the final compensated pattern to the initial uncompensated image shows that the pattern is modified by the algorithm over a much larger area than is originally affected by the defect, meaning it is the unwanted effects of the compensation features, not that defect, that need to be suppressed in the final iterations.

Looking at the final image in Figure 13, it is clear that the image is not perfect. There is an obvious dip in intensity near the defect. This is not surprising because the algorithm did not attempt to correct the image intensity in the center of the line, it only corrected the thresholded image. This simple algorithm is just an example of the power of fast simulation when applied to compensation. In the future, work will be done to develop a more sophisticated algorithm to compensate for buried defects near arbitrary patterns through focus and dose.

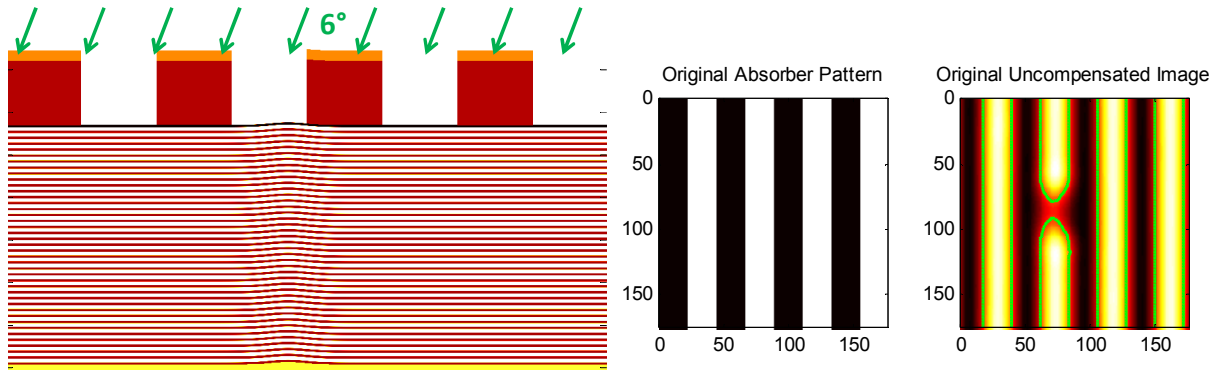


Figure 12. Defective mask geometry to be compensated for and original defective image. 22 Dense Lines, 3nm tall 65nm FWHM substrate defect, uniform defective layers from substrate to surface, Centered 22nm from the shadowed absorber edge. Axis unit are nm 1x wafer scale.

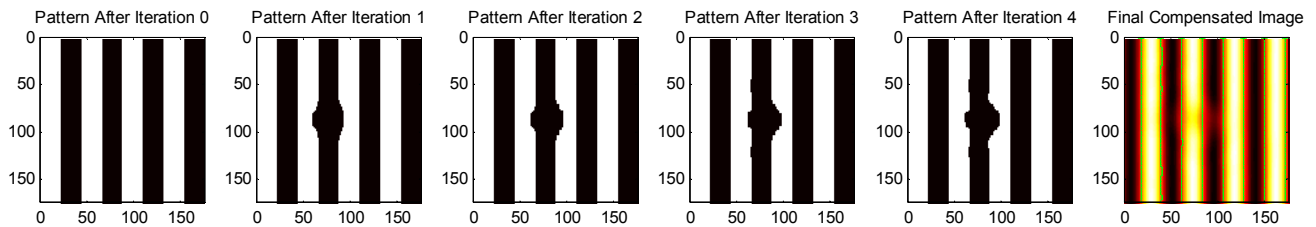


Figure 13. Pattern after each step of compensation algorithm along with the final image. Axis units are nm 1x wafer scale.

7. CONCLUSION

A new method for predicting the reflection from an extreme ultraviolet (EUV) multilayer was described which when implemented into the new Defect Printability Simulator (DPS) can calculate the image produced by an EUV mask with a buried defect several orders of magnitude faster than the finite difference time domain (FDTD). Also, a new buried defect compensation method was demonstrated to correct the in focus image of a line space pattern containing a buried defect.

The new multilayer model accounts for the disruption of the magnitude and phase of the reflected field from an EUV multilayer defect. It does this by sampling the multilayer on a non-uniform grid and calculating the analytic local reflection coefficient at each point. After this step, the effect of the optical path difference due to the surface defect profile is added to the total reflected field.

The accuracy of the new multilayer model and the full DPS simulator was verified by comparisons to FDTD simulations. The largest difference between the two methods was 0.8nm for predicting the CD change due to a buried defect through focus. This small difference is within the margin of error for FDTD simulations of EUV multilayers. The speed of DPS is compared to extrapolated FDTD runtimes for many simulation domain sizes and DPS is 4-5 orders of magnitude faster for all cases.

The new compensation strategy demonstrated in this work is able to remove all simulated CD error due to a buried defect in a 22nm dense line space pattern. The method is iterative and a full DPS simulation is run for every iteration. After each simulation, the absorber pattern is adjusted based on the difference of the thresholded target image and defective image. This method is very simple and does not attempt to compensate for the defect through focus, but it does demonstrate the usefulness of a fast simulator for defect compensation.

8. REFERENCES

-
- [1] C. H. Clifford, A. R. Neureuther, "Fast simulation methods and modeling for extreme ultraviolet masks with buried defects", *J. Micro/Nanolith. MEMS MOEMS* 8, 031402 (2009).
 - [2] Lam, M.C., et al., "Modeling methodologies and defect printability maps for buried defects in EUV mask blanks," *Proc. SPIE* 6151, (2007).
 - [3] Gullikson, E. M., et al. "Practical approach for modeling extreme ultraviolet lithography mask defects," *J. Vac. Sci. Technol. B* 20, 81 (2002).
 - [4] C. H. Clifford, "Simulation and Compensation Methods for EUV Lithography Masks with Buried Defects", Ph.D. Dissertation, Department of Electrical Engineering and Computer Sciences, University of California-Berkeley, (2010).